

## Central Lancashire Online Knowledge (CLOK)

Title	Triazine containing N-rich microporous organic polymers for CO <sub>2</sub> capture and unprecedented CO <sub>2</sub> /N <sub>2</sub> selectivity
Type	Article
URL	<a href="https://clock.uclan.ac.uk/id/eprint/17256/">https://clock.uclan.ac.uk/id/eprint/17256/</a>
DOI	<a href="https://doi.org/10.1016/j.jssc.2017.01.001">https://doi.org/10.1016/j.jssc.2017.01.001</a>
Date	2017
Citation	Bhunja, Subhajit, Bhanja, Piyali, Das, Sabuj Kanti, Sen, Tapas and Bhaumik, Asim (2017) Triazine containing N-rich microporous organic polymers for CO <sub>2</sub> capture and unprecedented CO <sub>2</sub> /N <sub>2</sub> selectivity. <i>Journal of Solid State Chemistry</i> , 247. pp. 113-119. ISSN 0022-4596
Creators	Bhunja, Subhajit, Bhanja, Piyali, Das, Sabuj Kanti, Sen, Tapas and Bhaumik, Asim

It is advisable to refer to the publisher's version if you intend to cite from the work.  
<https://doi.org/10.1016/j.jssc.2017.01.001>

For information about Research at UCLan please go to <http://www.uclan.ac.uk/research/>

All outputs in CLOK are protected by Intellectual Property Rights law, including Copyright law. Copyright, IPR and Moral Rights for the works on this site are retained by the individual authors and/or other copyright owners. Terms and conditions for use of this material are defined in the <http://clock.uclan.ac.uk/policies/>

# Triazine containing N-rich microporous organic polymers for CO<sub>2</sub> capture and unprecedented CO<sub>2</sub>/N<sub>2</sub> selectivity<sup>†</sup>

Subhajit Bhunia<sup>a</sup>, Piyali Bhanja<sup>a</sup>, Sabuj Kanti Das,<sup>a</sup> Tapas Sen,<sup>b</sup> and Asim Bhaumik<sup>a\*</sup>

<sup>a</sup>*Department of Material Science, Indian Association for the Cultivation of Science, Jadavpur, Kolkata - 700032, India*

<sup>a</sup>*Nanobiomaterials Research Group, Centre for Materials Science, School of Physical Sciences and Computing, University of Central Lancashire, Preston, PR1 2HE, UK*

\*Address for correspondence. Email: msab@iacs.res.in

<sup>†</sup>Electronic supplementary information (ESI) available: BET specific surface area plot, thermal stability of SB-TRZ-CRZ and SB-TRZ-TPA, synthetic procedures, <sup>13</sup>C and <sup>1</sup>H NMR spectra.

---

## Abstract

Targeted synthesis of microporous adsorbents for CO<sub>2</sub> capture and storage is very challenging in the context of remediation from green house gases. Herein we report two novel N-rich microporous networks SB-TRZ-CRZ and SB-TRZ-TPA by extensive incorporation of triazine containing tripodal moiety in the porous polymer framework. These materials showed excellent CO<sub>2</sub> storage capacities: SB-TRZ-CRZ displayed the CO<sub>2</sub> uptake capacity of 25.5 wt% upto 1 bar at 273 K and SB-TRZ-TPA gave that of 16 wt% under identical conditions. The substantial dipole quadrupole interaction between network (polar triazine) and CO<sub>2</sub> boosts the selectivity for CO<sub>2</sub>/N<sub>2</sub>. SB-TRZ-CRZ has this CO<sub>2</sub>/N<sub>2</sub> selectivity ratio of 377, whereas for SB-TRZ-TPA it was 97. Compared to other porous polymers, these materials are very cost effective, scalable and very promising material for clean energy application and environmental issues.

---

*Keywords:* CO<sub>2</sub> capture; CO<sub>2</sub>/N<sub>2</sub> selectivity; porous organic polymers; N-rich frameworks.

## **1. Introduction**

Climate change is a burning issue for our ecosystem and human beings due to tremendous emission of flue gas as a consequence of the industrial revolution [1]. The concentration of greenhouse gases (GHGs) such as CO<sub>2</sub>, CH<sub>4</sub>, NO<sub>x</sub> are ascending day by day, which is primarily responsible for global warming [2]. Flue gas from coal powder holds roughly 12 to 15 wt% CO<sub>2</sub> at 40 °C temperature. Carbon di oxide is the predominant component of flue gas, which absorbs considerable amount of the solar heat energy and thus creates a barrier for the heat energy to leave the atmosphere [3]. Hence CO<sub>2</sub> concentration is a potent menacing factor for the future of the earth. In this context carbon capture and storage (CCS) is an excellent technology to capture, compression and permanent storage of CO<sub>2</sub> from power plants, oil refineries and heavy chemical industries [4]. There are some difficulties in this technology like requirement of shared vision, international collaboration among governments. The post combustion type conventional technology uses amine absorber and the cryogenic cooler to separate CO<sub>2</sub> from the flue gas [5] but the amine scrubber needs more energy requirement, which makes the method less energy-efficient. The dimensions of various GHGs are relatively small, which makes the separation procedure difficult. But the difference in electronic property of the gases and that of the adsorbents are the key factor for selective separation. CO<sub>2</sub> has higher quadruple moment over N<sub>2</sub> which makes the selective adsorption of CO<sub>2</sub> over N<sub>2</sub> [6]. The proper tuning of molecular level is very essential for the CO<sub>2</sub> capture because only this type of strategy can take the advantage of chemical reactivity differences of the gas molecules.

Solid porous adsorbents are very demanding in the context of energy and environmental research. Huge numbers of microporous and mesoporous inorganic or organic-inorganic hybrid materials have been reported for CO<sub>2</sub> storage. From the inorganic platform, functionalized materials such as polyethylene amine tethered periodic MCM-41, polyaziridine coated silica, iridium complex etc. shows excellent efficiency for CO<sub>2</sub> uptake [7], but lack of stability is the key issue for this class of materials. Metal organic frameworks (MOFs) are known as the predominant member for the CO<sub>2</sub> storage material [8] because of their two or three dimensional porous framework with large accessible surface areas and huge pore volume. On the other hand, a wide range of crosslinked porous organic polymers bearing active functional groups has been developed in recent times and they have huge potential in selective gas adsorption [9].

Recently Yaghi et al. have carried out the interior modification of IRMOF-74-III by amino group to produce IRMOF-74-III-CH<sub>2</sub>NH<sub>2</sub>, which act as an excellent hybrid adsorbent for selective adsorption of CO<sub>2</sub> under humid conditions [10]. Many triazole based MOF structures modified with amine functionality [11], zeolitic imidazolate frameworks [12], acrylamide anchored MOFs [13] etc. are reported for efficient scaffold for reversible CO<sub>2</sub> storage. High surface area, presence of N-donor sites and tunable pore size are responsible for reversible CO<sub>2</sub> storage and higher CO<sub>2</sub>/N<sub>2</sub> selectivity. However, major drawback of the MOF material is the difficulty in their synthesis in the large scale to meet the industry demand. Pure microporous carbon based materials such as covalent organic framework (COFs) [14], porous organic polymers [15], hypercrosslinked polymers (HCPs) [16], resins [17] N-doped microporous carbon [18], POFs [19] etc. have shown tremendous potential in the CO<sub>2</sub> storage applications. Further, it is very challenging to control the organic building block in the porous structure to enhance the adsorption capacity and the selectivity of CO<sub>2</sub>. Chen et al. have reported the microporous

polycarbazole [20] of very high surface area together with very good CO<sub>2</sub> storage capacity. Mu et al. have reported carbazole based material MFCMP-1 [21] through an easy one step polymerization process, which showed a remarkable CO<sub>2</sub> storage capacity. Related porous polymers like PAF [22], FCDTPA [23] etc. have also the remarkable CO<sub>2</sub> uptake efficiency. Covalent triazine functionalized conjugated framework is also another important class of materials for selective CO<sub>2</sub> adsorption [24]. Zhou et al. have highlighted a highly porous host PPN and subsequent introduction of polar group in order to enhance the CO<sub>2</sub> uptake capacity [25]. These materials are advantageous over MOFs, silica, alumina based material because they have very high physicochemical stability with permanent porosity, highly scalable and can be synthesized without using any expensive catalyst or sophisticated techniques etc. Porous adsorbent having high CO<sub>2</sub> storage capacity and high CO<sub>2</sub>/N<sub>2</sub> selectivity are very demanding in the context of separation of flue gas mixture and thus boosting the isotheric heat of adsorption by increasing the CO<sub>2</sub>-philicity of porous solid adsorbent is very challenging.

Herein, we report a new strategy for maximum incorporation of N-containing polar functionality by using triazine containing trimodal crosslinker in polycarbazolic (Scheme 1, A<sub>1</sub>+B<sub>1</sub>, SB-TRZ-CRZ) and poly triphenylamine (Scheme 1, A<sub>1</sub>+B<sub>2</sub>, SB-TRZ-TPA) networks. We have modified the typical methodology of Lewis acid catalyzed Friedel-Craft reaction and these materials showed large reversible CO<sub>2</sub> uptake. To the best of our knowledge these materials displayed unprecedented CO<sub>2</sub>/N<sub>2</sub> selectivity among all HCPs. This can be attributed to high BET surface area and the presence of high density triazine moieties (N-rich centers) in the framework. These porous polymers are thoroughly characterized and their selective CO<sub>2</sub> capture application has been explored.

## 2. Experimental Section

## 2.1. Chemicals

4-(Bromomethyl)benzonitrile, carbazole, triphenylamine were purchased from Sigma Aldrich, India. Triflic acid was purchased from spectrochem, India. Anhydrous  $\text{AlCl}_3$  and all other remaining organic solvents were taken from E-Merck, India and used without further purification. 2,4,6-Tris[4-(bromomethyl)phenyl]-1,3,5-triazine was synthesized by the previously reported procedure (ESI S1).

## 2.2. Material Characterization

$^1\text{H}$  and  $^{13}\text{C}$  NMR studies were carried out using Bruker DPX-300 NMR spectrometer. Carbon, hydrogen and nitrogen contents of SB-TRZ-CRZ and SB-TRZ-TPA were evaluated by Perkin Elmer 2400 Series II CHN analyzer. X-Ray powder diffraction patterns of the samples were obtained with a Bruker AXS D8 Advanced SWAX diffractometer using  $\text{Cu K}\alpha$  ( $= 0.15406$  nm) radiation. Volumetric nitrogen adsorption/desorption experiments, Brunauer–Emmett–Teller (BET) specific surface area, pore volume and micropore analysis etc were carried out at 77 K using Autosorb 1 (Quantachrome, USA).  $\text{CO}_2$  adsorption/desorption experiments at of the materials was recorded by using a Bel Japan Inc. Belsorp-HP at 273 K and room temperature. Prior to adsorption measurement the samples were degassed in vacuum at  $140^\circ\text{C}$  for about 5 h. NLDFT pore-size distributions were obtained from the adsorption/desorption isotherms by using the carbon/slit-cylindrical pore model. The  $^{13}\text{C}$  cross-polarization magic angle spinning (CP-MAS) NMR spectrum was obtained on a 500 MHz Bruker advance II spectrometer at a mass frequency of 8 kHz. Thermogravimetry analysis (TGA) and differential thermal analyses (DTA) of the samples were carried out in a TGA Instruments thermal analyzer TA-SDT Q-600. A Hitachi S-5200 field-emission scanning electron microscope was used for the determination of the morphology of the particles. Transmission electron microscopy (TEM) images were obtained

using a JEOL JEM 2010 transmission electron microscope operating at 100 kV. The samples were prepared by dropping a colloidal solution onto the carbon-coated copper grids followed by drying under high vacuum. The  $^1\text{H}$  and  $^{13}\text{C}$  NMR spectra were obtained from Bruker AVANCE III-400 MHz spectrometer.  $^1\text{H}$  NMR spectra were collected at 400 MHz with chemical shift referenced to the residual peak in  $\text{CDCl}_3$  ( $\delta$ : H 7.26ppm. Multiplicities are written as s (singlet), d (doublet), t (triplet), m (multiplet) and br (broad). The Clausius–Clapeyron equation was used to calculate the enthalpies of adsorption for  $\text{CO}_2$  for SB-TRZ-CRZ and SB-TRZ-TPA. In each case, the data were obtained using the equation:  $(\ln P)_n = - (Q_{\text{st}}/R)(1/T) + C$ , where P indicates pressure, n is the adsorbed amount, T for temperature, R is the universal gas constant and C is a constant. The isosteric heat of adsorption  $Q_{\text{st}}$  was calculated from the slope of plots of  $(\ln P)_n$  as a function of  $1/T$ .

### 2.3. Synthesis of SB-TRZ-CRZ

Triazine containing microporous polymer was synthesized by using the Friedel-Crafts alkylation reaction between 2,4,6-tris[4-(bromomethyl)phenyl]-1,3,5-triazine ( $\text{A}_1$ ) and carbazole ( $\text{B}_1$ ). In a typical synthesis 2,4,6-tris[4-(bromomethyl)phenyl]-1,3,5-triazine (1.17g, 2 mmol) and carbazole (0.25g, 1.5 mmol) were mixed in anhydrous DCM. Then 0.8g of anhydrous  $\text{AlCl}_3$  was added to that solution and the mixture turned into red. It was then stirred at room temperature for 2 h under  $\text{N}_2$  atmosphere. Then the temperature was raised to  $80^\circ\text{C}$  and refluxed for 18h. The precipitate was then filtered and washed by plenty of methanol using a Soxhlet apparatus. The material was washed by acetone, THF, hexane successively and then pale greenish colored material (SB-TRZ-CRZ) obtained, which was dried under high vacuum for overnight. The yield of the reaction was 89% (1.26 g).

## 2.4. Synthesis of SB-TRZ- TPA

This material was synthesized by the same procedure described above using 2,4,6-tris[4-(bromomethyl)phenyl]-1,3,5-triazine (1.17g, 2 mmol) (A<sub>1</sub>) and triphenylamine (0.49 g, 2 mmol) (B<sub>2</sub>). The yield of the reaction is ~92 % (1.5 g).

## 3. Result and Discussion

C<sub>3</sub> symmetric tri-podal building block is very attractive for synthesizing polymeric porous frameworks. Here a triazine containing tripodal cross-linker has been used to knit the N-containing aromatics in the polymer network. Lewis acid catalyzed Friedel-Craft alkylation reaction, a well established protocol has been employed to form hypercrosslinked microporous structure with permanent and stable porosity. Several attempts had been made to introduce the polar functionality in the network in order to achieve higher CO<sub>2</sub> storage capacity. Here this cross-linker has a higher reactivity than other conventional ones due to triazine's electron withdrawing effect. This tripodal electrophile acts a doping agent of triazine in the polymeric network. Anhydrous aluminium chloride is used as a catalyst to make those materials. We had picked anhydrous FeCl<sub>3</sub> for this alkylation reaction but it led to the generation of undesired iron nanoparticle entrapped in the framework. AlCl<sub>3</sub> catalyzed reaction between 2,4,6-tris(4-(bromomethyl)phenyl)-1,3,5-triazine (TRZ) and carbazole (CRZ) has produced the greenish yellow thick mass and subsequent filtration and several washing by methanol, acetone and THF gave the greenish yellow light weighted powder of SB-TRZ-CRZ and the reaction between TRZ and triphenylamine (TPA) gave the brown material SB-TRZ-TPA after filtration and repeated washing with different organic solvent. These materials are not soluble in any common organic solvents.



In order to obtain the bonding and structural information of SB-TRZ-CRZ and SB-TRZ-TPA at the molecular level, FT-IR and  $^{13}\text{C}$  CP/MAS NMR spectroscopic data had been recorded. The strong absorption at  $1513\text{ cm}^{-1}$  for SB-TRZ-CRZ and the peak at  $1509\text{ cm}^{-1}$  for SB-TRZ-TPA indicates the presence of triazine unit in the porous framework [26]. The peak at  $1361\text{ cm}^{-1}$  (SB-TRZ-CRZ) and  $1360\text{ cm}^{-1}$  (SB-TRZ-TPA) are for in plane stretching vibration of triazine ring. Peaks at  $805\text{ cm}^{-1}$  (SB-TRZ-CRZ) and  $815\text{ cm}^{-1}$  (SB-TRZ-TPA) could be attributed to the breathing vibration for the triazine ring. There is no prominent peak in the range of  $500\text{--}700\text{ cm}^{-1}$ , which confirmed that complete condensation of the monomers has been achieved (Figure 1).  $^{13}\text{C}$  cross polarization magic angle spinning (CP-MAS) NMR had been taken to estimate the structural integrity of two type of porous framework. SB-TRZ-CRZ and SB-TRZ-TPA showed the peak at  $\sim 168\text{ ppm}$ , a characteristic peak of  $\text{sp}^2$  carbon of triazine unit [27]. The peaks near  $148$  and  $109\text{ ppm}$  for SB-TRZ-CRZ are the indicative for the two carbazolic carbon, respectively for [f] and [g]. The various carbons come from the triazinyl phenyl unit and carbazolic unit, are responsible for the most intense peak at  $129\text{ ppm}$  which is shown in the Figure 2 (down). SB-TRZ-TPA showed an intense peak at  $130\text{ ppm}$  with a small hump at  $136\text{ ppm}$ , respectively and these are assigned to the phenyl ring of triphenylamine and triazine substituted phenyl ring as shown in the Figure 2 (up). The peak corresponding to benzylic carbon for SB-TRZ-CRZ is at  $\sim 40\text{ ppm}$  and for SB-TRZ-TPA at  $\sim 38\text{ ppm}$  [28], can be attributed to different electronic effect of carbazole and triphenylamine upon  $\text{C}_3$  symmetric tris-crosslinker. Both materials are purely amorphous in nature and did not show any peak in wide angle X-ray powder diffraction. The thermal stability of SB-TRZ-CRZ and SB-TRZ-TPA has been estimated by thermogravimetric analysis (TGA). It revealed that SB-TRZ-TPA is thermally more stable than SB-TRZ-CRZ. SB-TRZ-TPA is quite stable upto  $400^\circ\text{C}$  and whereas SB-TRZ-CRZ undergoes roughly 5% weight

loss at nearly 150 °C due to loss of some solvent molecule or water entrapped in the network followed by structural cleavage above 300 °C. Thus, SB-TRZ-CRZ is stable upto 300 °C (ESI S4).

### 3.1. Porosity Measurement

The porous nature of the hypercrosslinked structure is revealed from the sorption analysis using N<sub>2</sub> gas as an adsorbate molecule. The N<sub>2</sub> adsorption/desorption isotherms are measured at 77 K is shown in the Figure 3 SB-TRZ-CRZ showed a typical type I isotherm, which suggested the pure microporous nature [29] of this carbazole based framework according to the IUPAC classification. SB-TRZ-TPA also displayed a type I nature in its adsorption/desorption isotherms. The Brunauer–Emmett–Teller (BET) specific surface area of SB-TRZ-CRZ is 642 m<sup>2</sup>g<sup>-1</sup> (ESI S5) and that of SB-TRZ-TPA is 310 m<sup>2</sup>g<sup>-1</sup> (Figure 3a). The pore size distribution of the two triazine based materials are calculated using the non-local density functional theory (NLDFT) theory and carbon slit pore model. The predominant pore sizes as estimated from the respective pore size distribution plots for these materials are 1.7 nm for SB-TRZ-CRZ and 1.5 nm for SB-TRZ-TPA, which suggested that both materials possess extremely large micropores/supermicropores (Figure 3b). The pore volumes of SB-TRZ-CRZ and SB-TRZ-TPA are 0.2888 and 0.1469 ccg<sup>-1</sup>, respectively (Table 1).

### 3.2. Microstructural Analysis

The particle morphology of the two networks is determined with the help of field emission scanning electron microscopic (FE-SEM) and high resolution transmission electron microscopic (HRTEM) analyses. FE-SEM images suggested particle morphology of microporous triazine knitted carbazole networks of SB-TRZ-CRZ is composed of submicron spheres of average diameter 350-450 nm (Figures 4a,b) at different magnification. SB-TRZ-TPA

is composed of small agglomerated inter grown particles with average diameter 450-600 nm (Figures 4c,d). High-resolution transmission electron microscopic (TEM) images of both these porous polymers indicated that they are composed of very tiny particles with interparticle void spaces (Figures 4e,f).

### 3.3. Reversible CO<sub>2</sub> Capture

Enhancing CO<sub>2</sub>-philicity of the porous network is a big challenge to increase the CO<sub>2</sub> uptake capacity. Recently it is reported that carbon based porous adsorbent should be functionalized in such way that the network will be able to create a pronounced magnetic field at the surface that CO<sub>2</sub> can interact extensively with the porous host via its quadrupole interaction [30]. Generally the presence of nitrogen atom in the carbon scaffold increases the affinity of the network towards CO<sub>2</sub> because of facilitated dipole-quadrupole interaction [31]. Several microporous polycarbazole, poly triphenylamine are known for good CO<sub>2</sub> storage material [32]. Here we have investigated the doping effect of triazine into porous N-containing microporous polymer and the change of the CO<sub>2</sub> storage efficiency using a triazine containing tripodal crosslinker. The loading of triazine moiety in the polycarbazole and polytriphenyl network has been optimized by using various molar ratios of the individual monomers. Faul et al. have synthesized several poly triphenylamine via Buchwald–Hartwig coupling having the CO<sub>2</sub> uptake capacity 6.5 wt% [33]. Dai et al. have synthesized various modified polycarbazoles such as (P-PCz) [34], TSP-1, TSP-2 etc in order to boost the CO<sub>2</sub> uptake capacity and the uptake capacities are respectively 5.57 mmol g<sup>-1</sup>, 18 wt%. Han et al. have synthesized the polycarbazole [35] (CPOP-16-19) having CO<sub>2</sub> uptake capacity of 16.7 wt% upto 1 bar 273 K.

Here we have incorporated triazine moiety in the N-containing porous polymeric backbones, which is very desirable for post combustion CO<sub>2</sub> capture application [36]. SB-TRZ-

CRZ has shown the 25.5 wt% CO<sub>2</sub> uptake upto 1 bar at 273 K and 44.5 wt % upto 3 bar at 273 K (Figure 5a). It also has shown remarkable CO<sub>2</sub> uptake upto 3 bar at room temperature [37] (13.9 wt%). SB-TRZ-TPA has shown 29.8 wt% CO<sub>2</sub> uptake upto 3 bar at 273 K and nearly 16 wt % (upto 1 bar) at 273 K (Figure 5c). SB-TRZ-TPA exhibits the CO<sub>2</sub> uptake of 11 wt% at room temperature (303 K) (Table 1). So it is clear that the method of doping of triazine into polycarbazole and poly triphenylamine in our work significantly effective toward CO<sub>2</sub> storage application. The CO<sub>2</sub> philicity of the polymeric network has tremendously increased from previously reported modified polycarbazole and polytriphenylamine. CO<sub>2</sub> uptakes of these two materials are also very comparable with previously best reported COFs [38,39], MOFs [40,41], N-doped microporous carbons [42,43], hypercrosslinked porous polymers [44-46] etc. The high density of basic nitrogen sites of triazine present in the polymer network which interact with Lewis acidic CO<sub>2</sub> molecules via dipole quadrupole interaction, are responsible for huge CO<sub>2</sub> uptake [47]. Further, large CO<sub>2</sub> uptake capacity for these materials can be attributed to the high degree of crosslinking between the monomers used to construct the hypercrosslinked structure which leads to high concentration of triazine and N-containing arenes in the network. The degree of elastic expansion of porous structure (swelling) creates the difference between the deformed pore volume and true pore volume which manifests in the N<sub>2</sub> adsorption/desorption isotherm at 77 K.

### **3.4. CO<sub>2</sub>/N<sub>2</sub> selectivity**

In spite of moderate surface area of SB-TRZ-CRZ and SB-TRZ-TPA they displayed huge CO<sub>2</sub> uptake and thus it is necessary to investigate the preferential uptake of CO<sub>2</sub> over N<sub>2</sub> to understand the efficacy of gas separation application. The selectivity of the gas uptake towards CO<sub>2</sub> over N<sub>2</sub> is measured by volumetric measurement of pure gas physisorption isotherm at 273

K. The microporous polymer having larger surface area will definitely have the higher CO<sub>2</sub> uptake capacity but it is very challenging to tune the organic building blocks of the polymeric network in such a way that CO<sub>2</sub> uptake capability will be much higher considering its relatively low surface area and thus those materials will come with a excellent selectivity of CO<sub>2</sub>/N<sub>2</sub>. As seen in Figures 5a and 5c, the CO<sub>2</sub> adsorption curves are following the linear trend with increasing the pressure whereas N<sub>2</sub> exhibited no significant uptake. SB-TRZ-CRZ has shown 5.7 mmol/g CO<sub>2</sub> uptake upto 1 bar at 273 K and ~10 mmol/g upto 3 bar. On the other hand SB-TRZ-TPA has shown 3.6 mmol/g CO<sub>2</sub> uptake upto 1 bar and 6.7 mmol/g upto 3 bar at 273 K. The CO<sub>2</sub>/N<sub>2</sub> selectivity has been calculated by taking the ratio of two initial slopes of the isotherms of CO<sub>2</sub> and N<sub>2</sub>. The calculated CO<sub>2</sub>/N<sub>2</sub> selectivity of SB-TRZ-CRZ and SB-TRZ-TPA are 377:1 (Figure 5b) and 97:1 (Figure 5d), , respectively at 273 K. As far as we know these selectivity values are precisely comparable with those of recently reported hypercrosslinked polymers (Th-1, Py-1, Fu-1 [48], anyline-benzene co-polymer network [49], hydroxyl containing MOPs [50]), COFs(ILCOF-1[51], 3D-Py-COF [52]), MOFs [53,54] and porous carbons [55]. By measuring the CO<sub>2</sub> adsorption isotherm at different temperature and applying Clausius-Claperyron equation, we have calculated isoelectric heat of adsorption, and corresponding values are in the range of 32-38 kJ/ mol for SB-TRZ-CRZ (Figure 6a) and 34-35 kJ/ mol for SB-TRZ-TPA (Figure 6b) which is higher than triazine based poly-benzimidazole (TBILP-1) [56] and comparable to ultramicroporous poly-benzimidazole (BILP-101) [57], recently reported hypercrosslinked polymer (Figure 7).

#### 4. Conclusion

Triazine functionalized two new microporous polymers SB-TRZ-CRZ and SB-TRZ-TPA have been synthesized by one step, easy Lewis acid catalyzed Friedel-Crafts alkylation reaction

using a triazine containing tripodal crosslinker, which knitted carbazole and triphenylamine molecules, and resulted efficient incorporation of triazine in polycarbazole and poly-triphenylamine networks. These materials have high BET surface areas  $642 \text{ m}^2\text{g}^{-1}$  (SB-TRZ-CRZ) and  $310 \text{ m}^2\text{g}^{-1}$  (SB-TRZ-TPA). The  $\text{CO}_2$  uptake capacity of SB-TRZ-CRZ is 25.5 wt% upto 1 bar at 273 K and SB-TRZ-TPA is 16 wt % under identical conditions. Selective gas adsorption analysis revealed that SB-TRZ-CRZ has a  $\text{CO}_2/\text{N}_2$  selectivity of 377 and SB-TRZ-TPA has the selectivity of 97. Synthesis of these novel hypercrosslinked microporous materials and their large carbon dioxide uptakes reported herein may contribute significantly in developing an efficient adsorbent for environmental remediation.

## **Acknowledgments**

SB and PB wish to thank CSIR, New Delhi and SKD wish to thank UGC, New Delhi for their respective Senior and Junior Research Fellowships. AB and TS wish to thank DST, New Delhi and British Council, UK for providing research grants through DST-UKIERI project.

## Notes and References

- [1] N. Y. Du, H. B. Park, M. M. Dal-Cin, M. D. Guiver, *Energy Environ. Sci.* **5** (2012) 7306-7322.
- [2] M. Meinshausen, N. Meinshausen, W. Hare, S. C. B. Raper, K. Frieler, R. Knutti, D. J. Frame, M. R. Allen, *Nature* **458** (2009) 1158-1162.
- [3] D. Aaron , C. Tsouris, *Separation Sci. Technol.* **40** (2005) 321-348.
- [4] M. E. Boot-Handford, J. C. Abanades, E. J. Anthony, M. J. Blunt, S. Brandani, N. Mac Dowell, J. R. Fernandez, M. C. Ferrari, R. Gross, J. P. Hallett, R. S. Haszeldine, P. Heptonstall, A. Lyngfelt, Z. Makuch, E. Mangano, R. T. J. Porter, M. Pourkashanian, G. T. Rochelle, N. Shah, J. G. Yao, P. S. Fennell, *Energy Environ. Sci.* **7** (2014) 130-189.
- [5] M. Mofarahi, Y. Khojasteh, H. Khaledi, A. Farahnak, *Energy* **33** (2008) 1311-1319.
- [6] Q. Q. Dang, Y. F. Zhan, X. M. Wang, X. M. Zhang, *ACS Appl. Mater. Interfaces* **7** (2015) 28452-28458.
- [7] N. D. McNamara, J. C. Hicks, *ChemSusChem* **7** (2014) 1114-1124.
- [8] A. R. Millward, O. M. Yaghi, *J. Am. Chem. Soc.* **127** (2005) 17998-17999.
- [9] D. M. D'Alessandro, B. Smit, J. R. Long, *Angew. Chem. Int. Ed.* **49** (2010) 6058-6082.
- [10] A. M. Fracaroli, H. Furukawa, M. Suzuki, M. Dodd, S. Okajima, F. Gándara, J. A. Reimer, O. M. Yaghi, *J. Am. Chem. Soc.* **136** (2014) 8863-8866.
- [11] J. -J. Hou, X. Xu, N. Jiang, Y. -Q. Wu, X. -M. Zhang, *J. Solid State Chem.* **223** (2015) 73-78.

- [12] R. Banerjee, A. Phan, B. Wang, C. Knobler, H. Furukawa, M. Ókeeffe, O. M. Yaghi, *Science* 319 (2008) 939-943.
- [13] B. Zheng, J. Bai, J. Duan, L. Wojtas, M. J. Zaworotko, *J. Am. Chem. Soc.* 133 (2011) 748-751.
- [14] R. Gomes, P. Bhanja and A. Bhaumik, *Chem. Commun.* 51 (2015) 10050-10053.
- [15] S. Ren , M. J. Bojdys , R. Dawson , A. Laybourn , Y. Z. Khimyak , D. J. Adams, A. I. Cooper, *Adv. Mater.* 24 (2012) 2357-2361.
- [16] S. Bhunia, B. Banerjee, A. Bhaumik, *Chem. Commun.* 51 (2015) 5020-5023.
- [17] A. P. Katsoulidis, M. G. Kanatzidis, *Chem. Mater.* 23 (2011) 1818-1824.
- [18] M. Nandi, K. Okada, A. Dutta, A. Bhaumik, J. Maruyama, D. Derks, H. Uyama, *Chem. Commun.* 48 (2012) 10283-10285.
- [19] A. P. Katsoulidis, S. M. Dyar, R. Carmieli, C. D. Malliakas, M. R. Wasielewski, M. G. Kanatzidis, *J. Mater. Chem. A* 1 (2013) 10465-10473.
- [20] Q. Chen, M. Luo, P. Hammershøj, D. Zhou, Y. Han, B. W. Laursen, C. –G. Yan, B. –H. Han, *J. Am. Chem. Soc.* 134 (2012) 6084-6087.
- [21] Y. Zhang, S. A, Y. Zou, X. Luo, Z. Li, H. Xia, X. Liu, Y. Mu, *J. Mater. Chem. A* 2 (2014) 13422-13430.
- [22] T. Ben, C. Pei, D. Zhang, J. Xu, F. Deng, X. Jing, S. Qiu, *Energy Environ. Sci.* 4 (2011) 3991-3999.
- [23] X. Yang, M. Yu, Y. Zhao, C. Zhang, X. Wang, J. –X. Jiang, *J. Mater. Chem. A* 2 (2014)



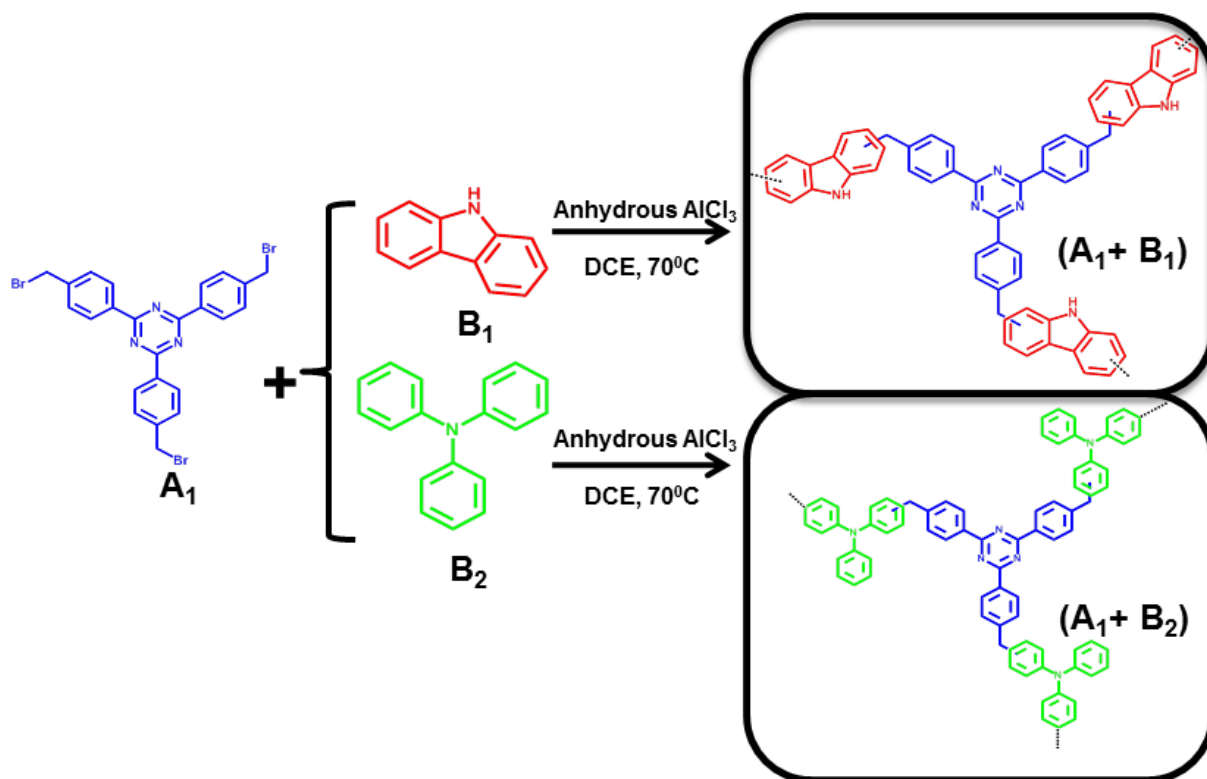
15139-15145.

- [24] X. Zhu, C. Tian, S. M. Mahurin, S. –H. Chai, C. Wang, S. Brown, G. M. Veith, H. Luo, H. Liu, S. Dai, *J. Am. Chem. Soc.* 134 (2012) 10478-10484.
- [25] W. Lu, D. Yuan, J. Sculley, D. Zhao, R. Krishna, H. –C. Zhou, *J. Am. Chem. Soc.* 133 (2011) 18126-18129.
- [26] W. Zhang, C. Li, Y. –P. Yuan, L. –G. Qiu, A. –J. Xie, Y. –H. Shen, J. –F. Zhu, *J. Mater. Chem.* 20 (2010) 6413-6415.
- [27] B. Jürgens, E. Irran, J. Senker, P. Kroll, H. Müller, W. Schnick, *J. Am. Chem. Soc.* 125 (2003) 10288-10300.
- [28] Y. Luo, S. Zhang, Y. Ma, W. Wang, B. Tan, *Polym. Chem.* 4 (2013) 1126-1131.
- [29] W. Lu, J. P. Sculley, D. Yuan, R. Krishna, Z. Wei, H. –C. Zhou, *Angew. Chem. Int. Ed.* 51(2012) 7480-7484.
- [30] P. Raveendran, Y. Ikushima, S. L. Wallen, *Acc. Chem. Res.* 38 (2005) 478-485.
- [31] M. Khajepour, J. F. Kauffman, *J. Phys. Chem. A* 104 (2000) 9512-9517.
- [32] F. Jiang, J. Sun, R. Yang, S. Qiao, Z. An, J. Huang, H. Mao, G. Chen, Y. Ren, *New J. Chem.* 2016 DOI: 10.1039/C5NJ03215F.
- [33] Y. Liao, J. Weber, C. F. J. Faul, *Chem. Commun.* 50 (2014) 8002-8005.
- [34] T. Jin, Y. Xiong, X. Zhu, Z. Tian, D. –J. Tao, J. Hu, D. Jiang, H. Wang, H. Liu, S. Dai, *Chem. Commun.* 52 (2016) 4454-4457.
- [35] L. Pan, Q. Chen, J. –H. Zhu, J. –G. Yu, Y. –J. He, B. –H. Han, *Polym. Chem.* 6 (2015)

2478-2487.

- [36] B. Li, Z. Zhang, Y. Li, K. Yao, Y. Zhu, Z. Deng, F. Yang, X. Zhou, G. Li, H. Wu, N. Nijem, Y. J. Chabal, Z. Lai, Y. Han, Z. Shi, S. Feng and J. Li, *Angew. Chem. Int. Ed.* 51 (2012) 1412-1415.
- [37] A. R. Millward, O. M. Yaghi, *J. Am. Chem. Soc.* 127 (2005) 17998-17999.
- [38] P. J. Waller, F. Gándara, O. M. Yaghi, *Acc. Chem. Res.* 48 (2015) 3053-3063.
- [39] Y. Zeng, R. Zou, Y. Zhao, *Adv. Mater.* 2016, DOI: 10.1002/adma.201505004.
- [40] D. Britt, H. Furukawa, B. Wang, T. G. Glover, O. M. Yaghi, *Proc. Natl. Acad. Sci. USA* 106 (2009) 20637-20640.
- [41] A. Aijaz, N. Fujiwara, Q. Xu, *J. Am. Chem. Soc.* 136 (2014) 6790-6793.
- [42] M. Sevilla, P. V. Vigón, A. B. Fuertes, *Adv. Funct. Mater.* (2011) 21 2781-2787.
- [43] W. Xing, C. Liu, Z. Zhou, L. Zhang, J. Zhou, S. Zhuo, Z. Yan, H. Gao, G. Wang, S. Z. Qiao, *Energy Environ. Sci.* 5 (2012) 7323-7327.
- [44] R. T. Woodward, L. A. Stevens, R. Dawson, M. Vijayaraghavan, T. Hasell, I. P. Silverwood, A. V. Ewing, T. Ratvijitvech, J. D. Exley, S. Y. Chong, F. Blanc, D. J. Adams, S. G. Kazarian, C. E. Snape, T. C. Drage, A. I. Cooper, *J. Am. Chem. Soc.* 136 (2014) 9028-9035.
- [45] M. G. Rabbani, T. E. Reich, R. M. Kassab, K. T. Jackson, H. M. El-Kaderi, *Chem. Commun.* 48 (2012) 1141-1143.
- [46] X. Jing, D. Zou, P. Cui, H. Ren, G. Zhu, *J. Mater. Chem. A* 1 (2013) 13926-13931.

- [47] R. Vaidhyanathan, S. S. Iremonger, G. K. H. Shimizu, P. G. Boyd, S. Alavi, T. K. Woo, *Science* 330 (2010) 650-653.
- [48] Y. Luo, B. Li, W. Wang, K. Wu, B Tan, *Adv. Mater.* 24 (2012) 5703-5707.
- [49] R. Dawson, T. Ratvijitvech, M. Corker, A. Laybourn, Y. Z. Khimyak, A. I. Cooper, D. J. Adams, *Polym. Chem.* 3 (2012) 2034-2038.
- [50] R. Dawson, L. A. Stevens, T. C. Drage, C. E. Snape, M. W. Smith, D. J. Adams , A. I. Cooper, *J. Am. Chem. Soc.* 134 (2012) 10741-10744.
- [51] M. G. Rabbani, A. K. Sekizkardes, Z. Kahveci, T. E. Reich, R. Ding, H. M. El-Kaderi, *Chem. Eur. J.* 19 (2013) 3324-3328.
- [52] G. Lin, H. Ding, D. Yuan, B. Wang, C. Wang, *J. Am. Chem. Soc.* 138 (2016) 3302-3305.
- [53] D. –M. Chen, N. Xu, X. –H. Qiu, P. Cheng, *Cryst. Growth Des.* 15 (2015) 961-965.
- [54] P. T. K. Nguyen, H. T. D. Nguyen, H. Q. Pham, J. Kim, K. E. Cordova, H. Furukawa, *Inorg. Chem.* 54 (2015) 10065-10072.
- [55] A. Modak, A. Bhaumik, *J. Solid State Chem.* 232 (2015) 157-162.
- [56] A. K. Sekizkardes, S. Altarawneh, Z. Kahveci, T. İslamoğlu, H. M. El-Kaderi, *Macromolecules* 47 (2014) 8328-8334.
- [57] A. K. Sekizkardes, J. T. Culp, T. Islamoglu, A. Marti, D. Hopkinson, C. Myers, H. M. El-Kaderi, H. B. Nulwala, *Chem. Commun.* (2015) 51 13393-13396.



**Scheme 1.** Preparation of triazine doped microporous organic polymer.

**Figure 1**

Bhunia et al.

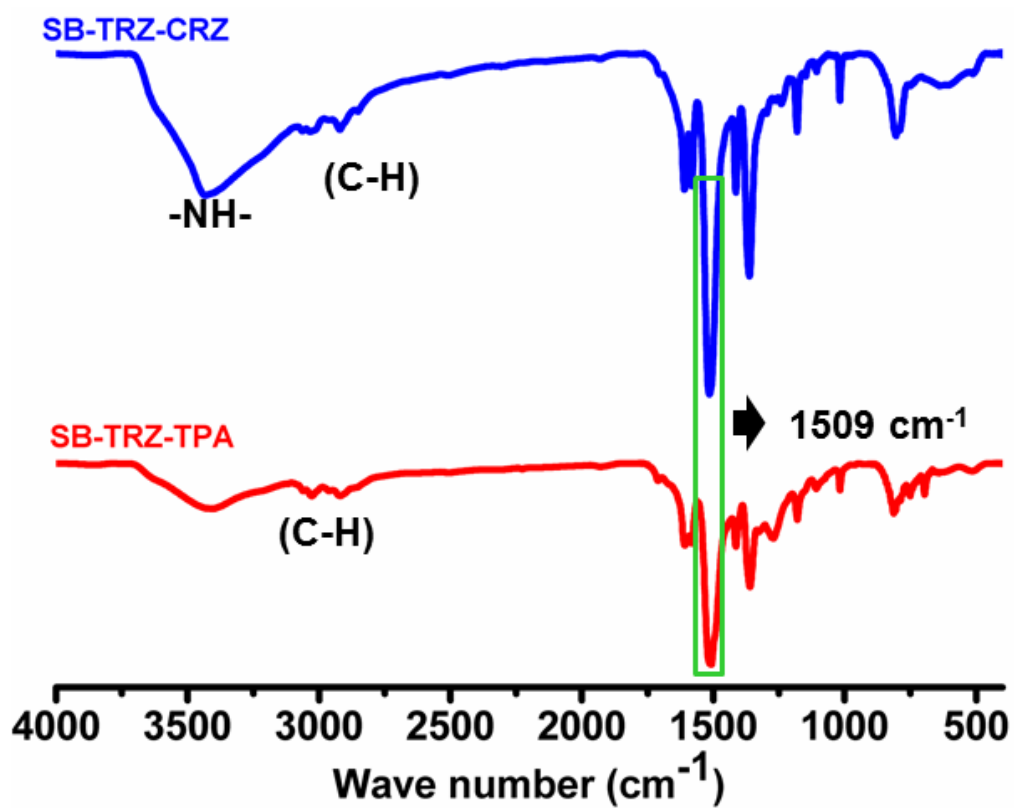


**Figure 1.** FT-IR spectra of SB-TRZ-CRZ and SB-TRZ-TPA

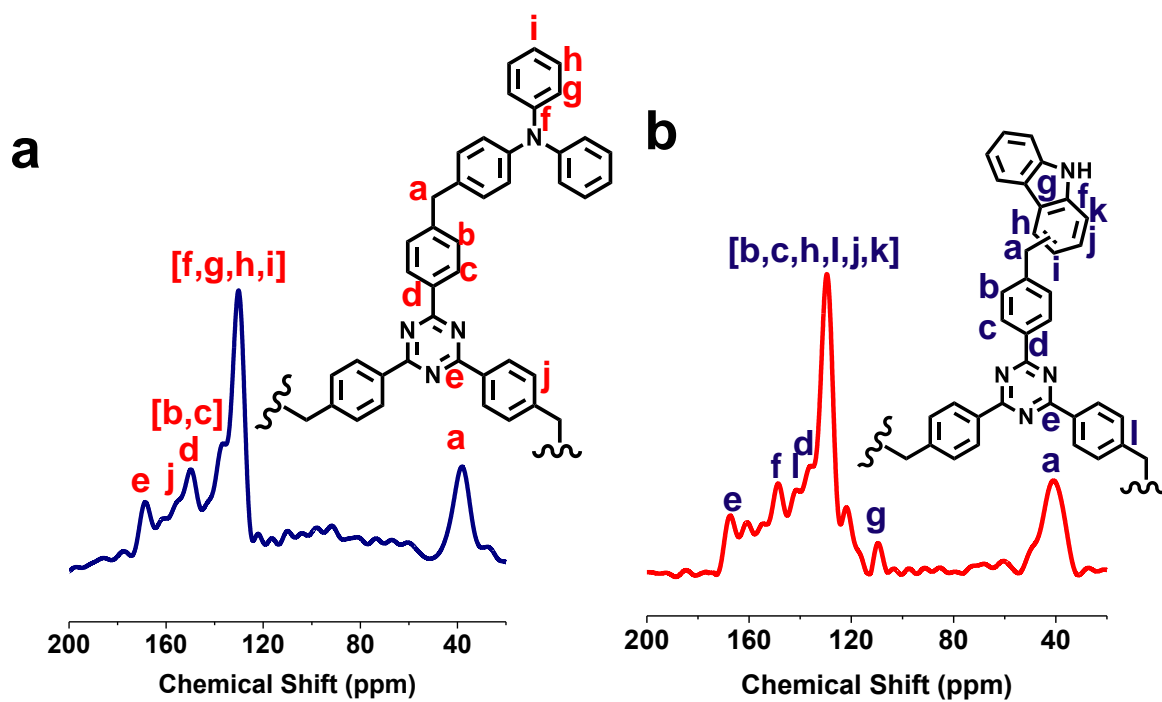


**Figure 2.** (a)(SB-TRZ-TPA (left, blue) (b) $^{13}\text{C}$  CP/MAS NMR spectra of SB-TRZ-CRZ (right, red, ) .

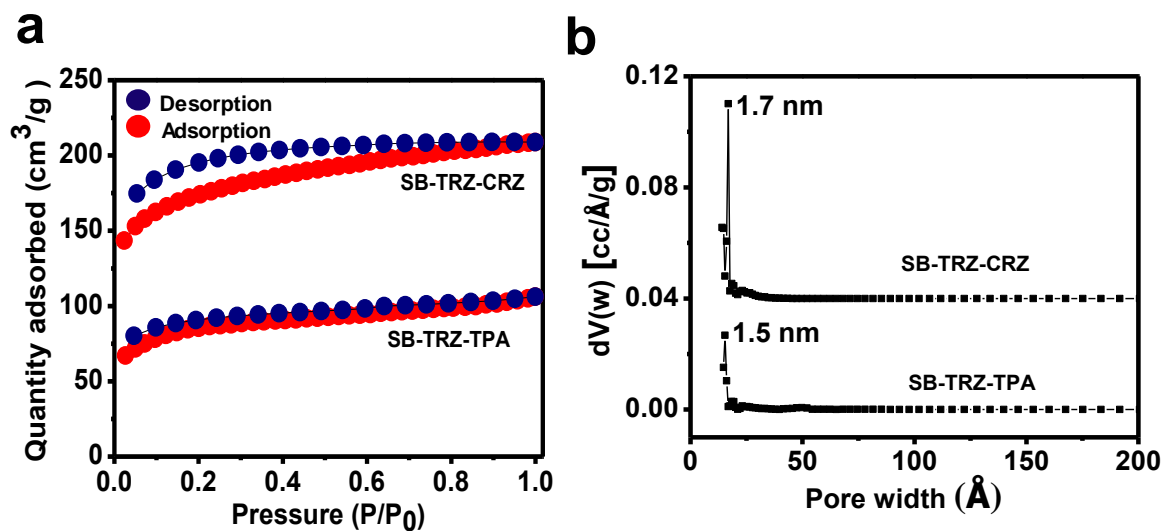


**Figure 3.** (a) N<sub>2</sub> adsorption/desorption isotherms of SB-TRZ-CRZ and SB-TRZ-TPA. Adsorption points are marked by red filled circle and desorption points by blue filled circle b) pore sized distribution of SB-TRZ-CRZ (upper) and SB-TRZ-TPA (lower) by NDLFT method.

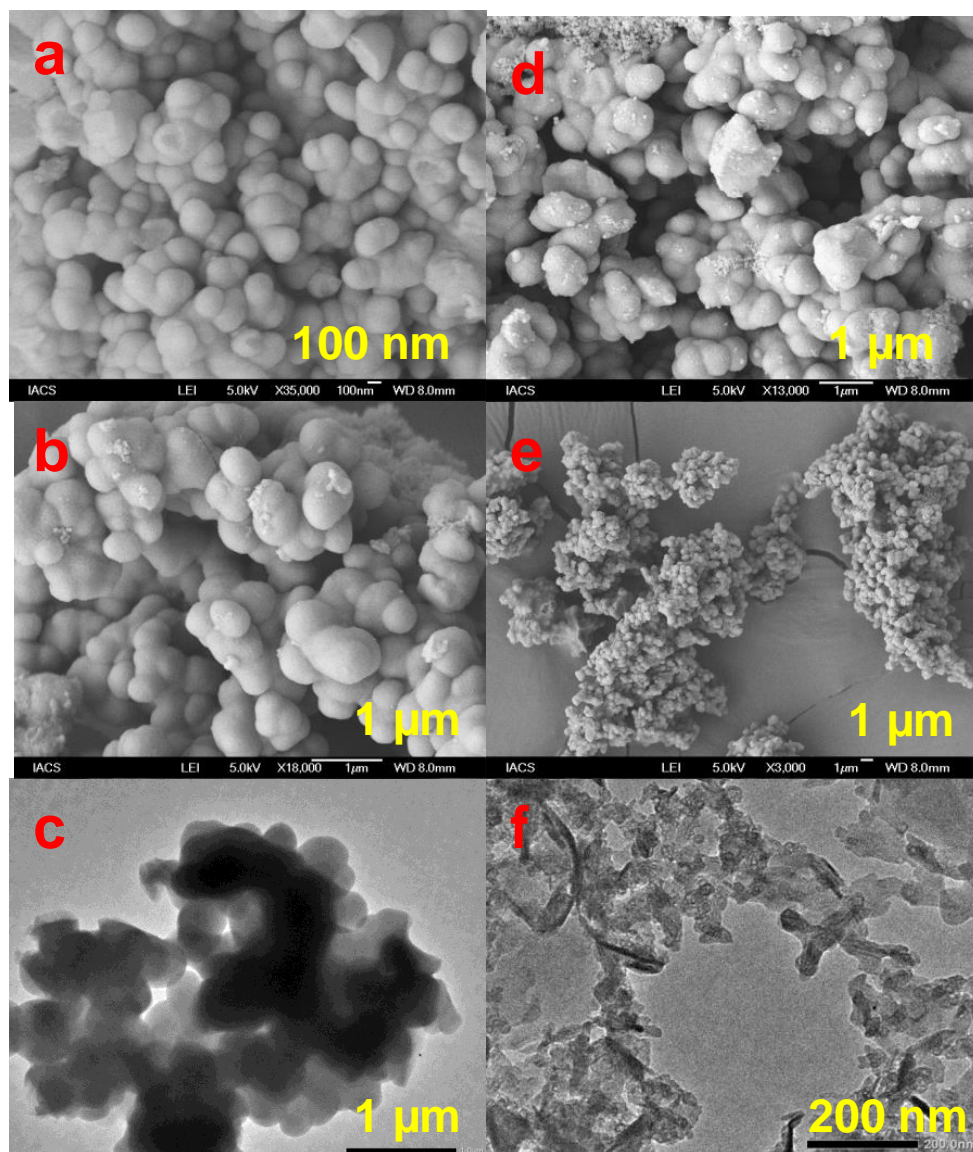


**Figure 4.** SEM images of SB-TRZ-CRZ at different magnification (a,b) and SB-TRZ-TPA (d,e); TEM image of SB-TRZ-CRZ (c) and SB-TRZ-TPA (f).



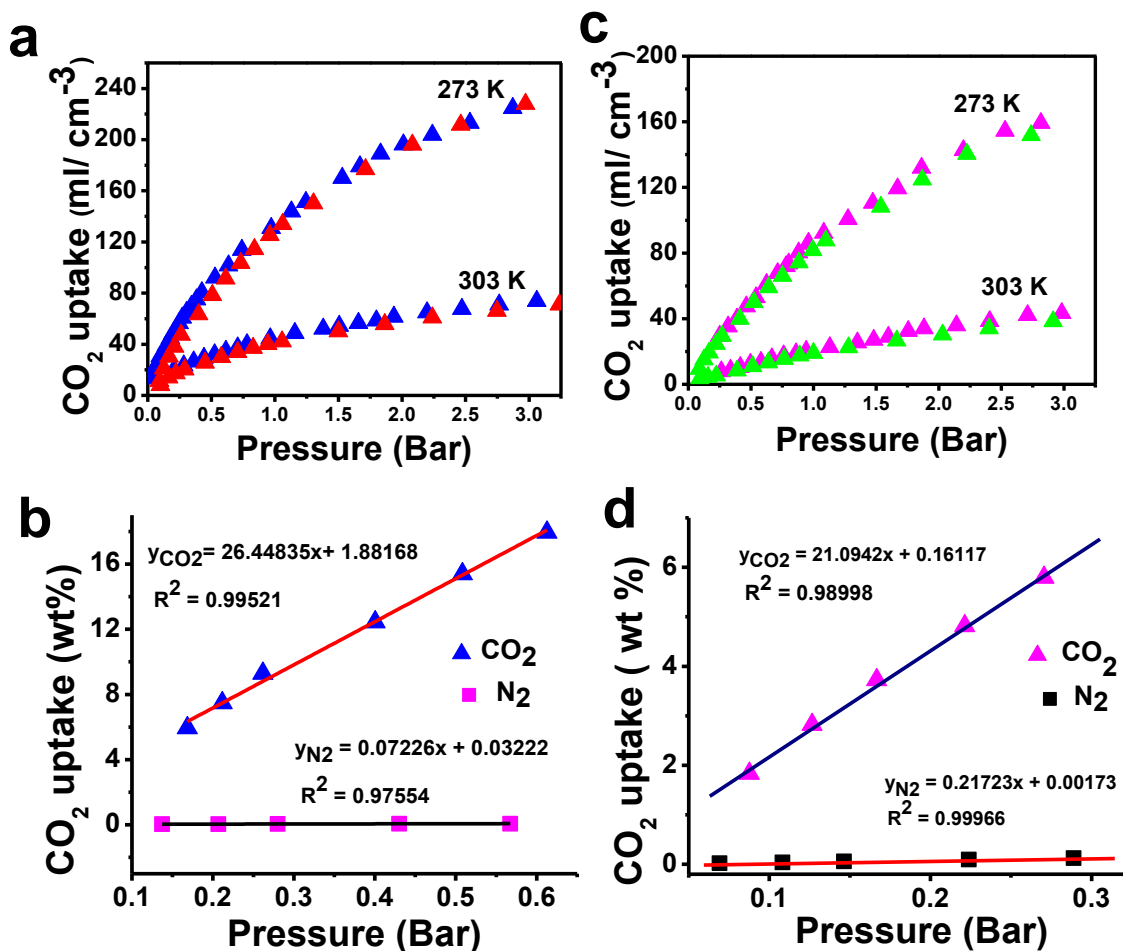


**Figure 5.** (a) CO<sub>2</sub> uptake of SB-TRZ-CRZ at 273 K and 303 K, (b) CO<sub>2</sub>/N<sub>2</sub> selectivity of SB-TRZ-CRZ, (c) CO<sub>2</sub> uptake of SB-TRZ-TPA at 273 K and 303 K, (d) CO<sub>2</sub>/N<sub>2</sub> selectivity of SB-TRZ-TPA.

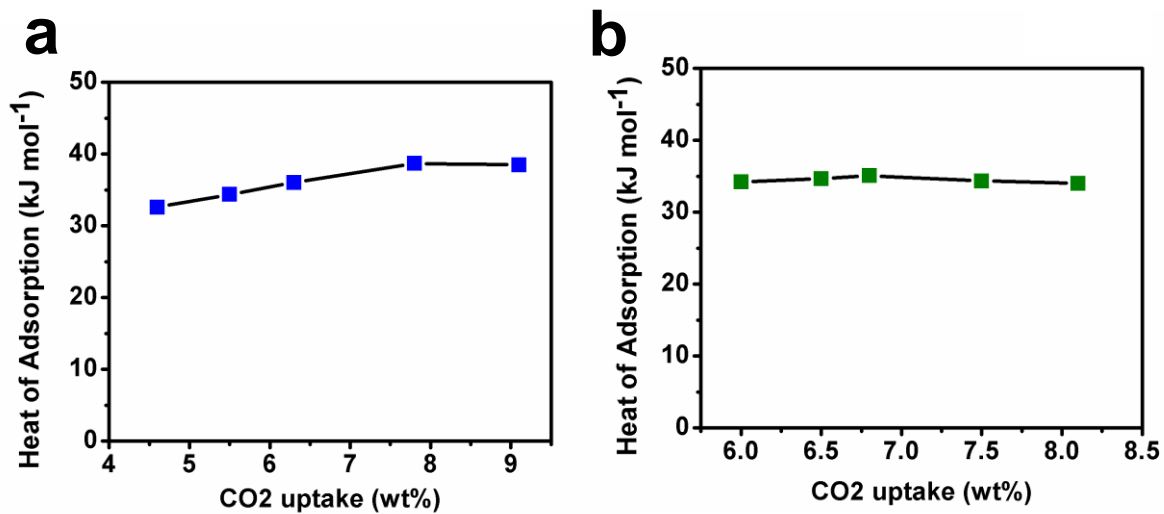


**Figure 6.** (a) isoelectric heat of adsorption of SB-TRZ-CRZ, (b) SB-TRZ-TPA.

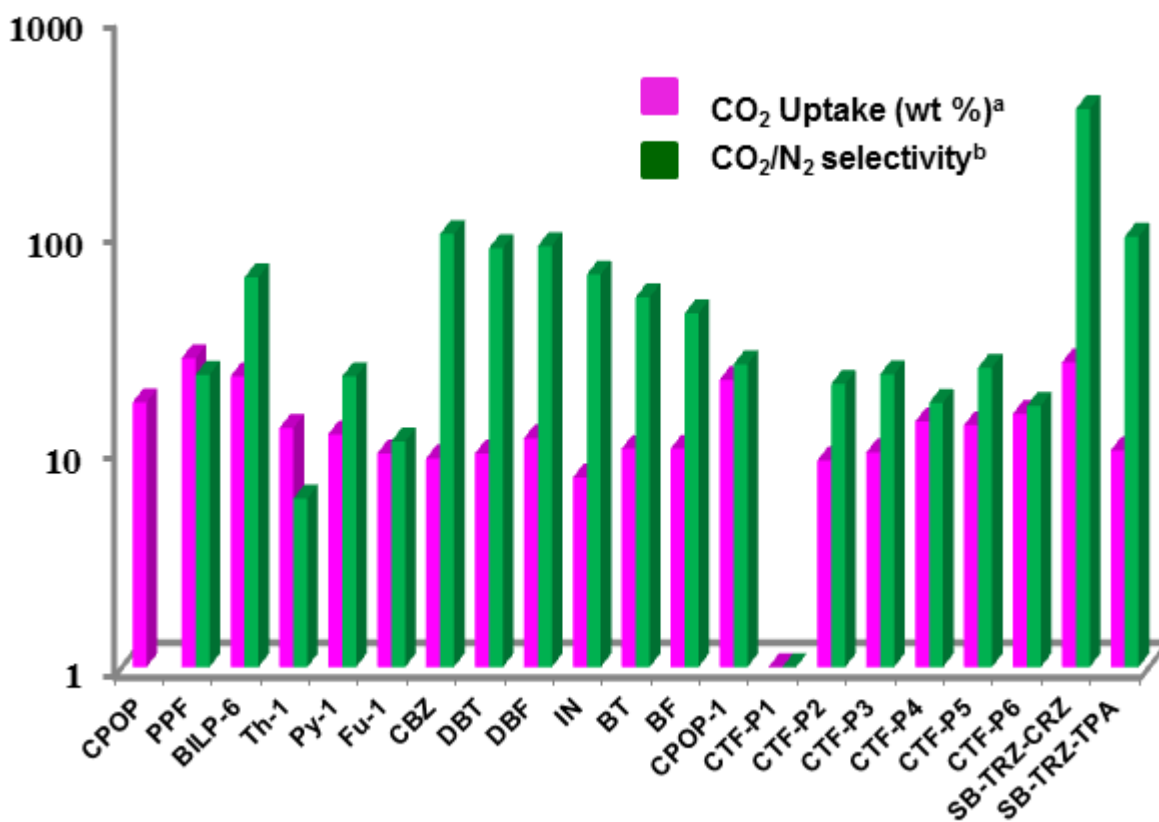


**Figure 7** logarithmic presentations of CO<sub>2</sub> uptake and selectivity (CO<sub>2</sub>/N<sub>2</sub>) of SB-TRZ-CRZ and SB-TRZ-TPA with recently reported organic microporous sorbents.<sup>48,50,51,52</sup>

<sup>a</sup> CO<sub>2</sub> uptake has been measured at 273 K and upto 1 atm

<sup>b</sup> selectivity of 273 K and it has been measured by taking the slope ration of two individual isotherms (CO<sub>2</sub> and N<sub>2</sub>)

**Table 1** Surface area, pore property and CO<sub>2</sub> upake efficiency of hypercrosslinked networks.

Material	S <sub>BET</sub> (m <sup>2</sup> /g)	Pore size (nm)	V <sub>total</sub> (cc/g)	CO <sub>2</sub> Uptake(wt%) (Upto 3 bar)		CO <sub>2</sub> /N <sub>2</sub> Selectivity <sup>a</sup> (273K)
				273K	298K	
<b>SB-TRZ- CRZ<sup>a</sup></b> (A1+B1)	642	1.7	0.2888	44.5	13.9	377:1
<b>SB-TRZ- TPA<sup>b</sup></b> (A1+B2)	330	1.5	0.1469	29.8	~ 11	97:1

<sup>a</sup>Ratio of A1:B1= 4:3

<sup>b</sup>Ratio of A1:B2= 1:1

<sup>a</sup>Selectivity was calculated by calculating the ratio of initial slope at low pressure region.